Reliability Evaluation of Rooftop Solar Photovoltaics Using Coherent Threshold Systems

Rudi Uswarman[1] and Ali Muhammad Rushdi[1*]

[1]*Department of Electrical and Computer Engineering, King Abdulaziz University, Jeddah 21589, Saudi Arabia.*

Authors' contributions

This work was carried out in collaboration between the two authors. Author RU performed the analysis, solved the example, wrote the first draft of the manuscript and initiated the literature search. Author AMR envisioned and designed the study, contributed to the symbolic and numerical analysis, checked the solution of the example, managed and finalized the literature search, and substantially edited and improved the entire manuscript. Both authors read and approved the final manuscript.

Article Information

Original Research Article

ABSTRACT

The trend for use of rooftop solar photovoltaics (PV) is rising due to their promising economic potential as a source of clean renewable energy. In general, a source of renewable solar energy consists of solar PV, an automatic charge controller, a battery pack, and an inverter. The reliability of a rooftop solar PV system is evaluated herein as that of a coherent threshold system (CTS). First, we utilize the unit-gap method and the fair-power method to verify that a given Boolean function is a threshold one and to identify its threshold and component weights. Both methods utilize specific features of the Karnaugh map (K-map). The unit-gap method uses the map to list all necessary inequalities by inspection, and then reduce them significantly by omitting dominated ones. The fair-power method uses the Karnaugh map to compute Banzhaf indices by appropriate map folding followed by XORing of true cells and false cells. We evaluate the CTS reliability via a recursive algorithm based on the Boole-Shannon's expansion in the switching domain, which is transformed via the real transform to the total probability law in the probability domain.

Corresponding author: Email: arushdi@yahoo.com;

1. INTRODUCTION

The term "Photovoltaics" (PV) denotes the conversion of sunlight or electromagnetic energy (in the frequency bands of visible and invisible light) into electrical energy using materials that exhibit the photovoltaic effect. The most familiar form of this effect uses solid-state semiconductor devices, mainly photodiodes. A solar photovoltaic system is considered a renewable energy source since its input (solar radiation or the radiation coming to earth from the sun) is not threatened by depletion within a human time scale. Currently, PV is one of the most effective alternative energy sources expected to meet electricity needs in high-temperature arid areas where intensive solar radiation might be optimally utilized. A solar PV system enjoys the prominent advantages of being low cost and pollution free. These advantages are causing an ongoing trend of a dramatic expansion of solar PV systems that is taking place at a rapid rate [1]. In the modern city, the positive trend of rooftop solar PV is rising due to the economic potential of solar energy [2-5]. The components of a rooftop solar PV system consist of solar PV, an automatic charge controller, a battery pack, and an inverter, with a configuration such as the one presented in Fig. 1. Solar PV panels installed on the roof of a house require an area around 10–12 m^2 to produce a power of 1 kW at noon in a sunny day at a moderate latitude. The solar panels are connected to an automatic charge controller, which serves to regulate the charging of the multiple batteries. A battery stores the electrical energy produced by the solar PV, and if the main

power source cannot meet the electricity needs, the battery will supply electricity through the inverter to convert the DC voltage into an AC voltage according to the specifications of the loads. The performance success or failure of a rooftop solar PV system, and hence its reliability, could be evaluated by modeling it as a coherent threshold system (CTS) [6].

This paper investigates the reliability of a rooftop solar PV system using the coherent threshold system (CTS) model. This model has been widely discussed and applied in several scientific fields [6-9]. The CTS model is also widely known in the open literature by the controversial name of a weighted k-out-of-n:G system [7], since it might be viewed as a non-symmetric extension of the partially-redundant system. The coherent threshold system is a coherent reliability system, whose success is a causal monotonically-increasing threshold switching function, for which no component is dummy or irrelevant [6-10]. A threshold switching function of n variables is characterized by $(n+1)$ real numbers: n weights W_i and a threshold T. The success of the system is satisfied if the total sum of the products $W_i X_i$ of a component success X_i by its weight W_i is equal to or larger than the threshold, and otherwise the system fails. Mathematically, this is stated as [6].

$$S(\mathbf{X}) = 1 \ iff \ \sum_{i=1}^{n} W_i X_i \geq T,$$

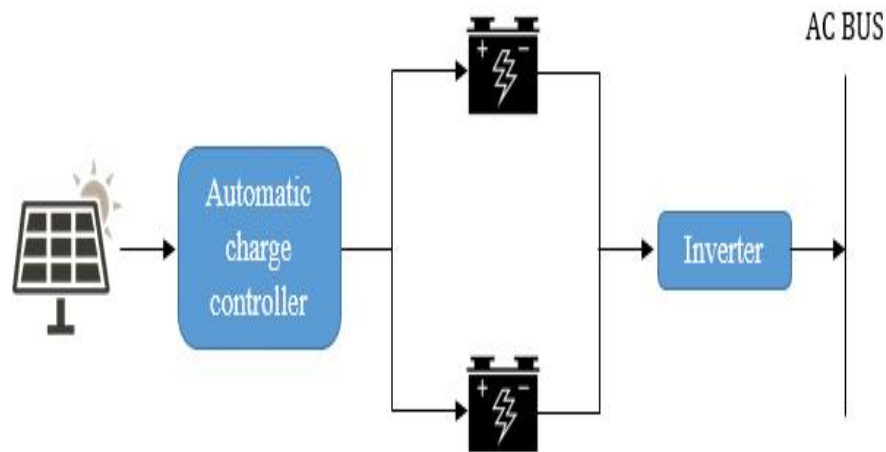and $\quad S(\mathbf{X}) = 0 \quad$ otherwise $\quad$ (1)

Fig. 1. Configuration of a solar PV system

2. METHODS AND RESULTS

The system success of the solar PV system under consideration is investigated via two techniques to verify that it is indeed a threshold switching function, and consequently to determine a specific (non-unique) set of values for the weights and threshold of this function. The techniques used are the unit-gap method and the fair-power method, adapted from Rushdi and Alturki [7]. These two techniques seem quite suitable among the plethora of existing methods for the synthesis of threshold Boolean functions. Once the threshold nature of the proposed system success is established and characterized, recursive relations and a recursion-based algorithm are forwarded for the reliability analysis of the corresponding CTS model [6-8].

2.1 The Unit-Gap Method

The unit-gap strategy is based on the construction of two forms or types of inequalities. The first type corresponds to the true vectors of the success function, in which the total sum of weighted successes of components is equal to or larger than the threshold ($\overrightarrow{W}^T\overrightarrow{X} \geq T$), and denoted to be such that ($S(\overrightarrow{X}) = 1$). By contrast, the second type of inequalities corresponds to the false vectors of the success function, in which the total sum of weighted successes of components is strictly lower than the threshold ($\overrightarrow{W}^T\overrightarrow{X} < T$), denoted as($S(\overrightarrow{X}) = 0$). In the unit-gap method, both the former non-strict inequalities and the latter strict ones are converted into appropriate equations. In fact, the former inequalities ($\overrightarrow{W}^T\overrightarrow{X} \geq T$) are satisfied exactly as equations ($\overrightarrow{W}^T\overrightarrow{X} = T$). while the latter inequalities ($\overrightarrow{W}^T\overrightarrow{X} < T$) are each subjected to a unit slack so as to be satisfied as equations ($\overrightarrow{W}^T\overrightarrow{X} = T - 1$). The true vectors are identified as cells belonging to the prime-implicant loops of the success function on the Karnaugh map (K-map), while the false vectors are recognized as cells found within the prime-implicate loops of this function on the K-map (which are the prime-implicant loops of system failure) .

The configuration of solar PV systems in Fig. 1 can be transformed into Fig. 2, which involves five components (X_1, X_2, X_3, X_4, X_5), whereX_1 is the success of the solar PV, X_2 is the success of the automatic charge controller, X_3 and X_4 are successes of the two batteries, and X_5 is the success of the inverter.

Fig. 2 depicts the logical (rather than physical) structure of the solar PV system. It could be used to write system success as a sum-of-products function (using and OR logic only) as shown in Eq. 2. The function in Eq. 2 is partially symmetric in elements X_1 , X_2, and X_5 . Itis also partially symmetric in elements X_3 and X_4 . Partially symmetric components can be interchanged with one another without affecting the success function

$$S(X_1, X_2, X_3, X_4, X_5) = X_1X_2X_5\,(X_3 \vee X_4) = X_1X_2X_3X_5 \vee X_1X_2X_4X_5. \qquad (2)$$

The success function of Eq. 2is analyzed by the K-map to get its prime-implicants and its prime implicates (complements of the prime implicants of the function's complement). We can find the prime implicants and prime implicates using properties of coherent functions, where a prime-implicant loop extends to the farthest cell from the all-true (all-1) cell and a prime-implicate loop extends to the farthest cell from the all-false (all-0) cells [7,11]. The prime implicants and the prime implicates of the system success are shown in Fig. 3 and Fig. 4, respectively. Based on Fig. 3 and Fig. 4, we can construct Fig 5,in which the yellow cells represent the farthest cells (from the all-1 cell) of the prime-implicant loops and the green cells represent the farthest cells (from the all-0 cell) of the prime-implicate loops. Rushdi and Alturki [7] have shown that inequalities corresponding to both types of colored cells dominate inequalities within the enclosing loops.

The inequalities of weights and threshold of the five-variable CTS model of the rooftop solar PV system are shown in Fig. 6. They consist of 32 inequalities (3 non-strict inequalities and 29 strict inequalities), and they involve 6 variables (5 weights and the threshold). Now, these 32 inequalities are reduced to just 6 dominating inequalities, which pertain to both types of colored cells in Fig. 5. Details of these 6 dominating inequalities of the system are explained in Table 1. In Table 1, the partial symmetry in X_3 and X_4mandates that (preferably) the parallel components 3 and 4 should have equal weights$W_3 = W_4$.There is another partial symmetry in X_1, X_2 and X_5, which necessitates that (preferably) the series components 1, 2, 5 should have the same weights. We will deliberately impose the first symmetry preferred requirement, but we will temporarily ignore the second. The last column of Table 1 shows that we now have 5 independent inequalities in 5 unknowns.

Based on Table 1, the non-strict inequalities are written as equalities shown in Eq. 3, and the strict inequalities are written as equalities (using a gap of unity) shown in Eq. 4

$$W_1 + W_2 + W_3 + W_5 = T, \qquad (3)$$

$$W_1 + W_2 + W_5 = W_1 + 2W_3 + W_5 = W_1 + W_2 + 2W_3 = W_2 + 2W_3 + W_5 = T - 1. \quad (4)$$

We can get $W_1 = 2$, $W_2 = 2$, $W_3 = W_4 = 1$, and $W_5 = 2$ by subtraction of each of the equations (4) from equation (3). Substitution of these values in any of the equations (3) or (4) yields $T = 7$. Finally, success in Eq. 1 can be satisfied with a threshold $T = 7$ and a weight vector $\vec{W} = [2\ 2\ 1\ 1\ 2]^T$. The fact that we ended with a solvable system of equations (3) and (4) verifies our underlying assumption that we are dealing with a threshold function, indeed. Though, we initially ignored the partial symmetry in components 1, 2, and 5, we were forced to recognize this symmetry by getting $W_1 = W_2 = W_5 = 2$. Had we recognized this symmetry from the outset, we would have imposed $W_1 = W_2 = W_5$ to replace (3) and (4) by

$$3W_1 + W_3 = T, \qquad (5a)$$

$$3W_1 = 2W_1 + 2W_3 = 2W_1 + 2W_3 = 2W_1 + 2W_3 = T - 1. \qquad (5b)$$

Equations (5) constitute 3 independent equations in 3 unknowns, which readily produce the same solution as above.

2.2 The Fair-Power Method

The fair-power method uses the Banzhaf indices as fair weights of the components of the rooftop solar PV system, whether system success is a threshold function or not. If later, we can identify an appropriate threshold value, then the system is a threshold one, indeed. A Banzhaf index [12-19] is defined as the number of true vectors (called weight or non-normalized syndrome) of the Boolean derivative with respect to the pertinent variable X_i. This derivative is obtained by XORing the two subfunctions/quotients/ratios obtained by restricting f to $X_i = 0$ and $X_i = 1$, respectively.

$$B_i = \text{weight}\left(\frac{\partial f}{\partial X_i}\right) = \text{weight}\left(f(X|\ X_i = 0 \oplus f X|\ Xi=1)\right) \qquad (6)$$

The Banzhaf indices of the components of the rooftop solar PV are illustrated in detail in Fig. 7,

where B_1, B_2, B_3, B_4, B_5 indicate the proposed weights of the components X_1, X_2, X_3, X_4 and X_5.

Fig. 7 shows the complete Banzhaf indexes of the components with weights of $W_1 = 3$, $W_2 = 3$, $W_3 = 1$, $W_4 = 1$, $W_5 = 3$. So far, we are not sure whether the success functionis threshold or not. We can assert that the function is a threshold one if we find a value T that fits as a threshold for it. We now construct a map for the pseudo-Boolean function

$$F_2(\vec{X}) = 3\ X_1 + 3\ X_2 + X_3 + X_4 + 3\ X_5, \qquad (7)$$

in which we weight every component success by the proposed weight or Banzhaf index in Fig. 8. In Fig. 8, we identify the 3 cells that must be true vectors (according to Fig. 3). Entries in these cells should be greater than or equal to T. In other words T is lower than or equal to the minimum entry in these cells, which is 10. Likewise, we identify the 29 cells that must be false vectors (according to Fig. 3). Entries in these cells should be strictly lower than T. In other words T is strictly greater than the maximum entry in these cells, which is 9. Any value in the semi-closed interval $(9,10]$ is acceptable for T, to render the system a threshold one. We choose $T = 10$ to secure a unit gap.

2.3 Recursive relations and algorithm

The Boole-Shannon expansion [6-9, 20-24] is useful to derive expressions for system success in the switching domain (two-valued Boolean domain), and expressions for system reliability in the probability domain. The reliability of the rooftop solar PV is obtained by the forthcoming Eq. 8, which is proposed in [6, 7], as an application of the Boole-Shannon to a threshold switching function, transformed to the probability domain.

$$R(n;\ \vec{p};\ \vec{W};T) = q_i R(n-1; \vec{p}/p_i; \vec{W}/W_i; T) + p_i R(n-1; \vec{p}/p_i; \vec{W}/W_i; T - W_i), \qquad (8)$$

$$R(n;\ \vec{p};\ \vec{W};T) = \begin{cases} 1 \text{ if } 0 \geq T \\ \text{if } \sum_{i-1}^{n} W_i < T \end{cases} \qquad (9)$$

The recursive relation in Eq. 8 must be supplemented by the boundary condition in Eq. 9. Here, the symbol $R(n;\ \vec{p};\ \vec{W};T)$ denotes the reliability (expectation of success) for a threshold system of n components with component reliabilities $\vec{p}$, and with weights $\vec{W}$ and a threshold

T. Based on Eq. 8 and Eq. 9, we can draw the signal flow graphs (SFGs) shown in Figs. 9-12. The black nodes in these figures are the sources of unit values, while the white nodes are fictitious or annihilating "sources" of zero values. Every non-source node has two arrows incident on it according to Eq. 8.

The signal flow graph is constructed with four different scenarios in Fig. 9-12. Fig. 9 and 11 use the worst policy (smallest weights first), while Fig. 10 and 12 employ the best policy (largest weights first). Fig. 9 and 10 employ the set of weights $[2\ 2\ 1\ 1\ 2]^T$ and the threshold T=7, while Figs. 11 and 12 employ the set of weights $[3\ 3\ 1\ 1\ 3]^T$ and the threshold T=10.

In the first scenario, components with the smallest weights are first used to decompose the success of the system. In the second scenario, components with the largest weights are first used to decompose the success of the system. The reliability according to the four scenarios in Figs. 9-12 are respectively

$$R(5;\vec{p};2,2,1,1,2;7) = p_1p_2p_3p_4p_5 + p_1p_2q_3p_4p_5 + p_1p_2p_3q_4p_5, \tag{10}$$

$$R(5;\vec{p};2,2,1,1,1,2;7) = p_1p_2p_4p_5 + p_1p_2p_3q_4p_5, \tag{11}$$

$$R(5;\vec{p};3,3,1,1,3;10) = p_1p_2p_3p_4p_5 + p_1p_2q_3p_4p_5 + p_1p_2p_3q_4p_5 \tag{12}$$

$$R(5;\vec{p};3,3,1,1,3;10) = p_1p_2p_4p_5 + p_1p_2p_3q_4p_5 . \tag{13}$$

The results in Eqs. 10 and 12 are identical and are shown on the Karnaugh map of Fig. 13, and the results in Eqs. 11 and 13 are identical and are shown on the Karnaugh map of Fig. 14.
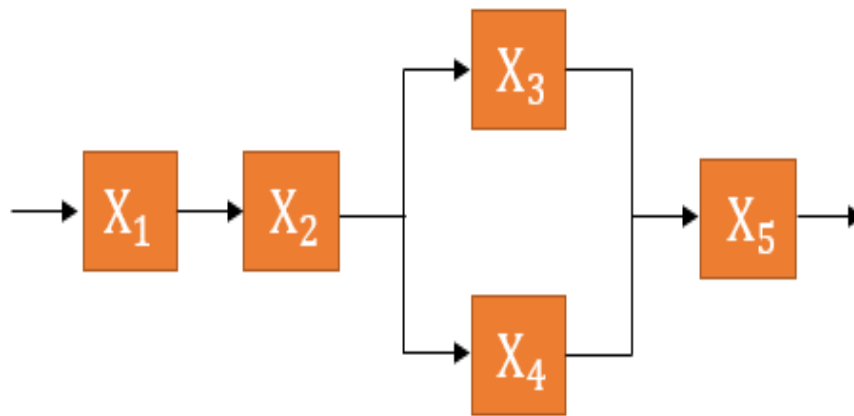

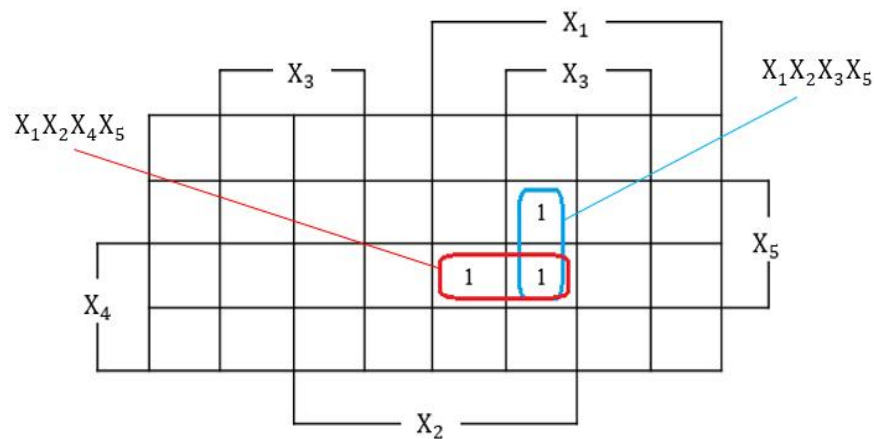**Fig. 2. Logical (rather than physical) structure of the solar PV system**

Fig. 3. Prime implicants for the success function in Eq. 1. These are the minimal paths of the logical configuration in Fig. 2
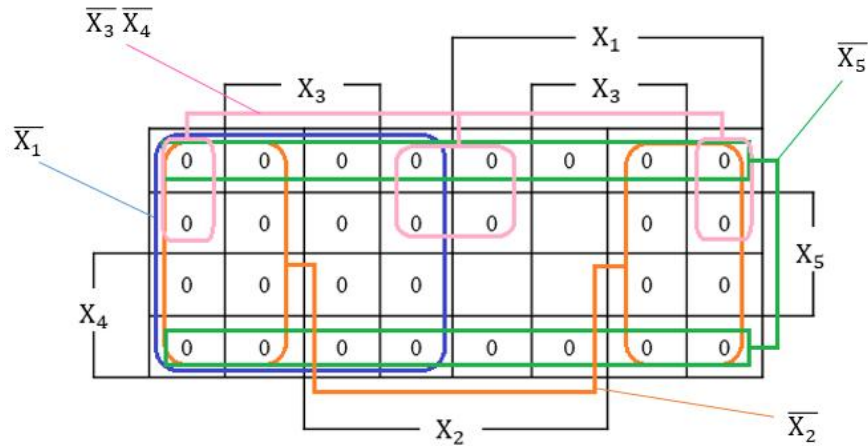
Fig. 4. Prime implicates for Eq. 1, denoted indirectly by their complementary values as the prime implicants of the complement of Eq. 1, i.e., of system failure. These latter entities (shown in figure) are the minimal cutsets of the logical configuration in Fig. 2
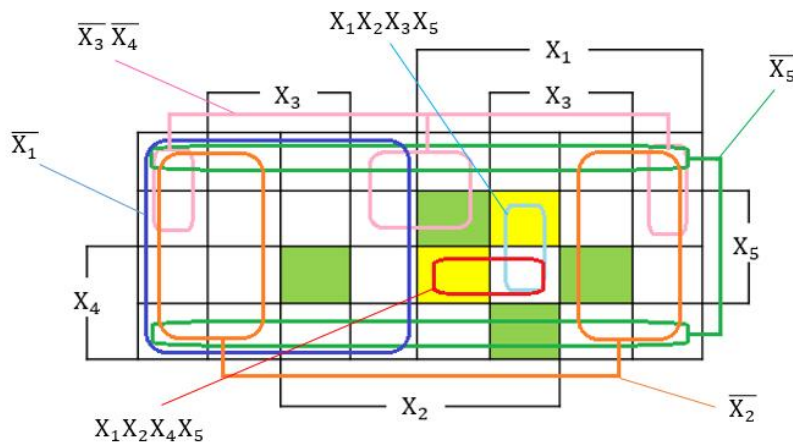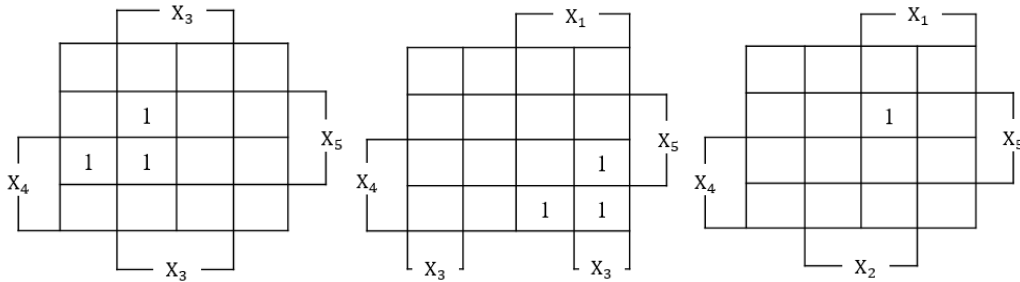

Fig. 5. Yellow cells represent prime-implicant locations (and green cells represent prime-implicates location) of the respective dominating inequalities
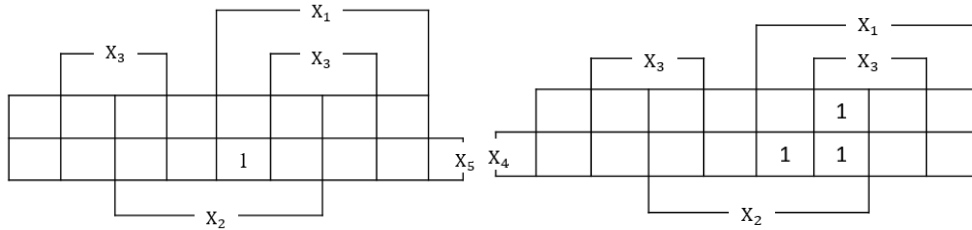

Fig. 6. The inequalities for the weights and threshold for Eq. 1

Table 1. Dominating inequalities

Dominating inequality	Exhausts	Symmetry of X_3 and X_4 only
True (On) cells		
$W_1 + W_2 + W_3 + W_5 \geq T$	A prime implicant	$W_1 + W_2 + W_3 + W_5 \geq T$
$W_1 + W_2 + W_4 + W_5 \geq T$	A prime implicant	$W_1 + W_2 + W_3 + W_5 \geq T$
False (Off) cells		
$W_1 + W_2 + W_5 < T$	A prime implicate	$W_1 + W_2 + W_5 < T$
$W_1 + W_3 + W_4 + W_5 < T$	A prime implicate	$W_1 + 2W_3 + W_5 < T$
$W_1 + W_2 + W_3 + W_4 < T$	A prime implicate	$W_1 + W_2 + 2W_3 < T$
$W_2 + W_3 + W_4 + W_5 < T$	A prime implicate	$W_2 + 2W_3 + W_5 < T$

$$B_1 = \text{weight}\left(\frac{\partial f}{\partial X_1}\right) = 3. \quad B_2 = \text{weight}\left(\frac{\partial f}{\partial X_2}\right) = 3. \quad B_3 = \text{weight}\left(\frac{\partial f}{\partial X_3}\right) = 1.$$

$$B_4 = \text{weight}\left(\frac{\partial f}{\partial X_4}\right) = 1. \quad B_5 = \text{weight}\left(\frac{\partial f}{\partial X_5}\right) = 3.$$
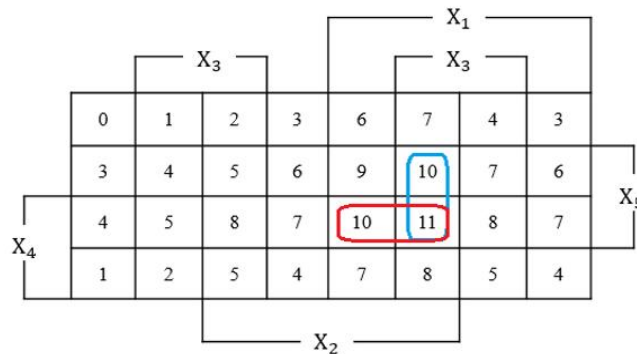
Fig. 7. Banzhaf indices for the function in Eq. 1

Fig. 8. Pseudo-Boolean function $F_2(\vec{X}) = 3X_1 + 3X_2 + X_3 + X_4 + 3X_5$, suggesting the feasibility of a threshold-function solution for the threshold $T = 10$
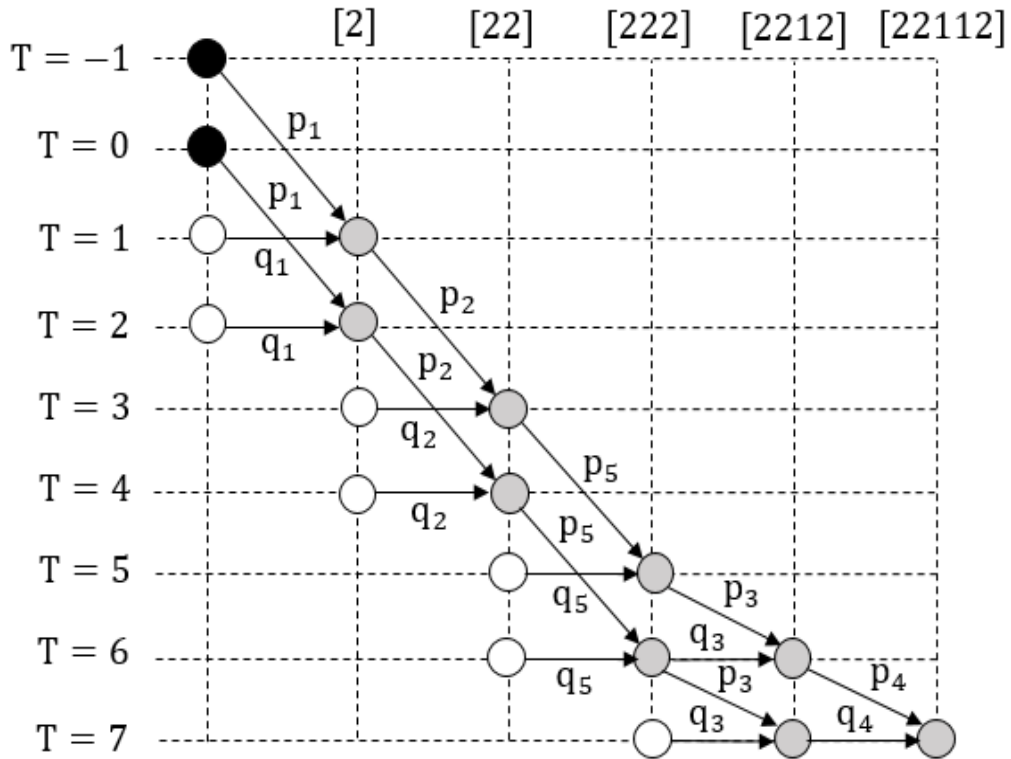
Fig. 9. Signal flow graph for worst-policy evaluation of system reliability with the set of weights [2 2 1 1 2]^T and the threshold T=7
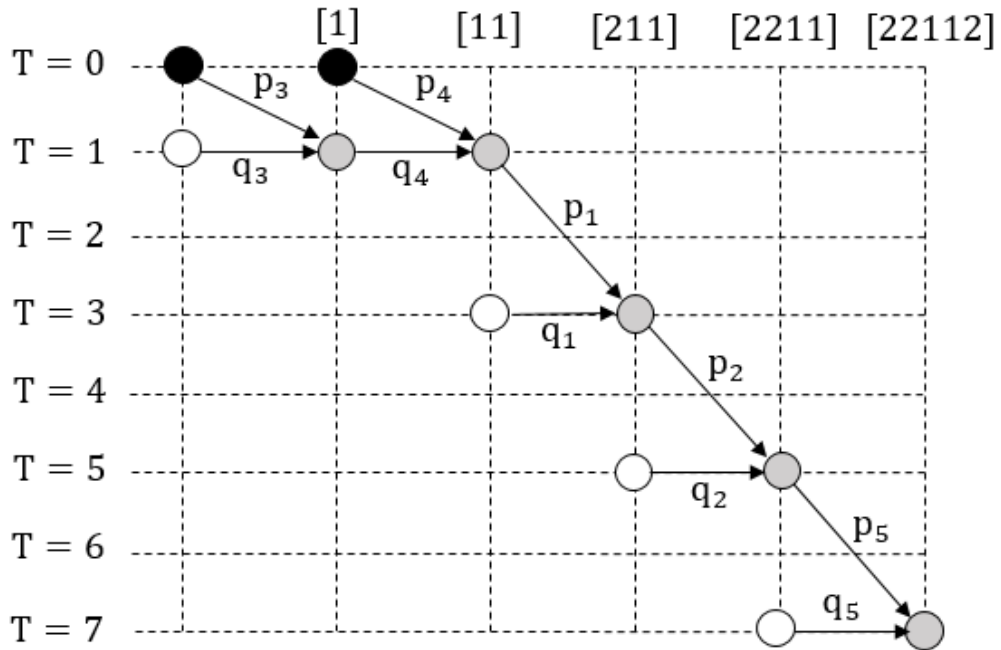

Fig. 10. Signal flow graph for best-policy evaluation of system reliability with the set of weights [2 2 1 1 2]^T and the threshold T=7
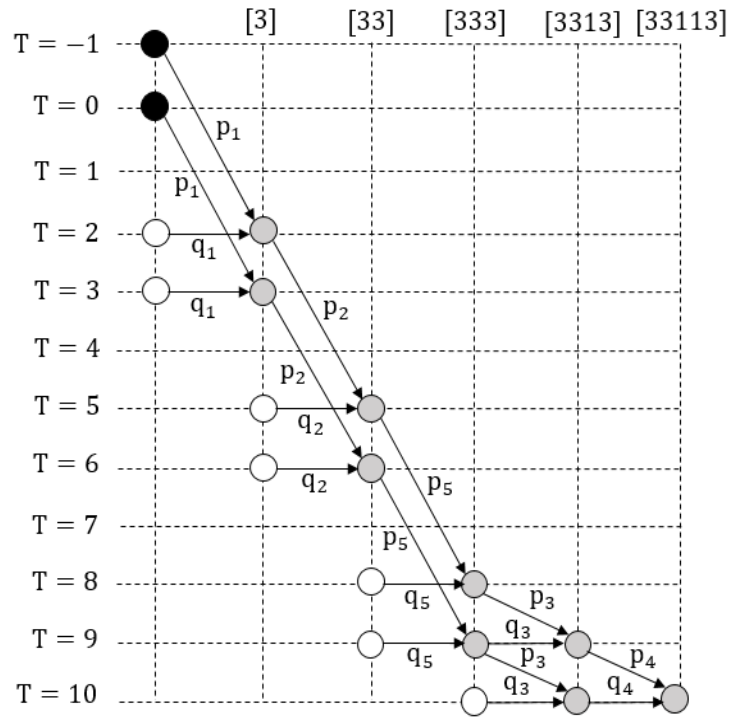
Fig. 11. Signal flow graph for worst-policy evaluation of system reliability with the set of weights [3 3 1 1 3]^T and the threshold T=10
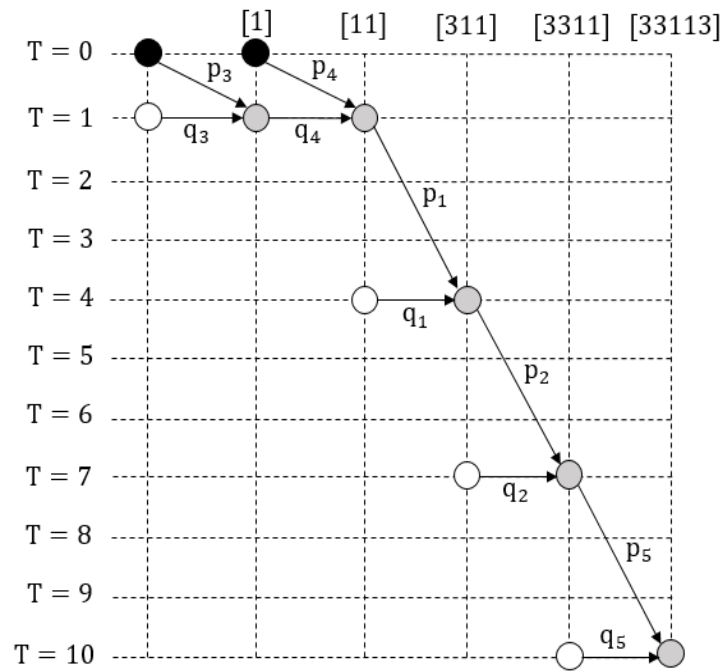

Fig. 12. Signal flow graph for best-policy evaluation of system reliability with the set of weights [3 3 1 1 3]^T and the threshold T=10
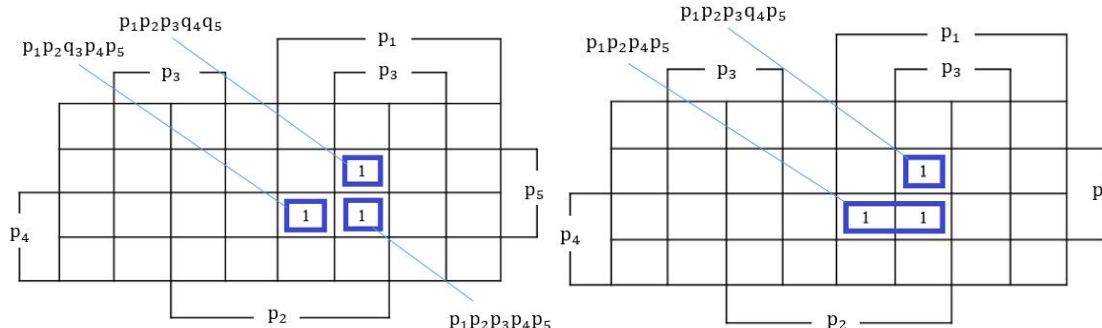
Fig. 13. The worst scenario for system reliability in Figs.9 and 11.   **Fig. 14. The best scenario for system reliability in Figs. 10 and 12.**

3. DISCUSSION

The reliability of rooftop solar PV systems are evaluated herein by the CTS technique. The weights and thresholds of the system success are defined via two methods. The first method is called the unit-gap method, while the second method is referred to as the fair-power method. The unit-gap method reduces the number of pertinent linear inequalities using domination among inequalities and symmetry of components. The fair-power method obtains the weights as Banzhaf indexes, and then fits an appropriate threshold with them. Subsequently, a recursive technique is used to derive a symbolic expression for the reliability of the pertinent CTS. The technique is illustrated by a probability map and an acyclic signal flow graph that resembles a reduced ordered binary decision diagram (ROBDD) [7, 8, 24-27]. Similar ROBDD-like SFGs were earlier employed for handling related systems [28-32]. The recursive algorithm has two different implementations that stand for two distinct strategies. It is a straightforward generalization of a recursive algorithm for computing the reliability of partially-redundant or k-out-of-n systems [33-36].The reliability results obtained herein are the same, despite the non-uniqueness for the threshold and weight values.

In passing, we note that there are many methods for the identification and synthesis of threshold Boolean functions [37-46], i.e., for determining whether a given Boolean (switching) function is threshold or not, and, if it is such, selecting appropriate (albeit non-unique) values for its weights and threshold. The two methods reported herein are just two representative methods that seem to be suitable for reliability applications pertaining to coherent threshold systems. We reiterate that threshold Boolean functions and coherent Boolean functions are two proper distinct subsets of unate Boolean functions [6]. Threshold Boolean functions might be coherent or non-coherent [6,30], and coherent Boolean functions might be threshold or non-threshold [7, 30]. The reader is referred to [30] for a taxonomy of CTS-related systems.

We have deliberately chosen the coherent-threshold model to address the general problem of reliability of photovoltaic systems. In retrospect, we note that this model is too powerful for the small example we elected to consider in this paper. Our example turned out to be a simple series-parallel system. It can be shown that a series-parallel system is a proper subset of the coherent threshold system [6]. In fact, it is shown in [6] that series systems and parallel systems are both threshold (and they are naturally coherent). Moreover, compositions of threshold and coherent systems are also threshold and coherent, respectively. Reliability analysis of series-parallel system is addressed by methods that are simpler and more efficient than those needed for more general systems [9, 20-22, 28, 47-53]. In fact, the main task in Boolean-based system reliability is to construct a probability-ready expression (PRE) [28]. The analyst is relieved of this major task when dealing with series-parallel systems since PREs are obtained for them merely by inspection [9, 28, 52, 53].

4. CONCLUSIONS

This paper investigated techniques for computing the reliability of a rooftop solar PV system using the coherent threshold system (CTS) model. Details for handling this model were given and its relation to other system models was briefly discussed.

COMPETING INTERESTS

The authors have declared that no competing interests exist.

REFERENCES

1. REN21. Renewables 2020 Global Status Report. REN21 Secretariat: Paris, France; 2020. Available:http://www.ren21.net/gsr-2020/
   accessed on 16 December 2020.
2. Saker N, Al-Qattan A, Al-Otaibi A, Al-Mulla A. Cost-benefit analysis of rooftop photovoltaic systems based on climate conditions of Gulf Cooperation Council countries, IET Renew. Power Gener. 2018;12(9):1074–1081.
   DOI: 10.1049/iet-rpg.2017.0309.
3. Senatla M, Bansal RC, Naidoo R, Chiloane L, Mudau U. Estimating the economic potential of PV rooftop systems in South Africa's residential sector: A tale of eight metropolitan cities, IET Renew. Power Gener. 2020;14(4):1–9.
   DOI: 10.1049/iet-rpg.2019.0946.
4. Coria G, Penizzotto F, Pringles R. Economic Analysis of Rooftop Solar PV Systems in Argentina, IEEE Lat. Am. Trans. 2020;18(1):32–42.
   DOI: 10.1109/TLA.2020.9049459.
5. Castellanos S, Sunter DA, Kammen DM. Rooftop solar photovoltaic potential in cities: How scalable are assessment approaches?, Environ. Res. Lett. 2017;12:12, ,
   DOI: 10.1088/1748-9326/aa7857.
6. Rushdi AM. Threshold systems and their reliability, Microelectron. Reliab. 1990;30:299-312.
7. Rushdi AMA, Alturki AM. Reliability of Coherent Threshold Systems, J. Appl. Sci. 2015;15(3):431–443,
   DOI: 10.3923/jas.2015.431.443.
8. Rushdi AM, Alturki AM. Novel representations for a coherent threshold reliability system: A tale of eight signal ow graphs, Turkish J. Electr. Eng. Comput. Sci. 2018;26(1):257–269.
   DOI: 10.3906/elk-1612-92.
9. Rushdi AMA, AK Hassan. An exposition of system reliability analysis with an ecological perspective, Ecol. Indic. 2016;63:282–295.
   DOI: 10.1016/j.ecolind.2015.11.050.
10. Ball MO, JS Provan. Disjoint products and efficient computation of reliability, Oper. Res. 1988;36:703-715.
11. Lee SC. Modern switching theory and digital design, Prentice-Hall, Englewood Cliffs, NJ., USA.
    ISBN-13: 97801355986806, pages: 498.
12. Banzhaf JF. Weighted voting doesn't work: A mathematical analysis, Rutgers Law Rev. 1964;19:317-343.
13. Dubey P, Shapley LS. Mathematical properties of the Banzhaf power index, Math. Oper. Res. 1979;4:99-131.
14. Rushdi AM. Map differentiation of switching functions. Microelectronics Reliability. 1986;26(5):891-908.
15. Yamamoto Y, Banzhaf index, Boolean difference. Proceedings of the 42nd IEEE International Symposium on Multiple-Valued Logic, Victoria, BC. 2012;191-196.
16. Alturki AM, Rushdi AM. Weighted voting systems: A threshold-Boolean perspective. Journal of Engineering Research. 2016;4(1):125-143.
17. Rushdi AM, Ba-Rukab OM. Calculation of Banzhaf voting indices utilizing variable-entered Karnaugh maps. Journal of Advances in Mathematics and Computer Science. 2017;20(4):1-17.
18. Rushdi AMA, Ba-Rukab OM. Translation of Weighted Voting Concepts to the Boolean Domain: The Case of the Banzhaf Index, Chapter 10 in Advances in Mathematics and Computer Science, Book Publishers International, Hooghly, West Bengal, India; 2019;122-140.
19. Muroga S. Logic design and switching theory, John Wiley and Sons, New York, USA; 1979.
    ISBN-13: 9780471625308.
20. Rushdi AM. Symbolic reliability analysis with the aid of variable-entered Karnaugh maps, IEEE Trans. Reliab. 1983;32(1):134-139.
21. AM Rushdi, Goda AS. Symbolic reliability analysis via Shannon's expansion and statistical independence," Microelectronics and Reliability. 1985;25(6):1041-1053.
22. AM Rushdi, Abdulghani AA. A comparison between reliability analyses based primarily on disjointness or statistical independence: The case of generalized Indra network, Microelectron. Reliab. 1993;33:965-978.
23. Rushdi AM, Ba-Rukab OM. A doubly-stochastic fault-tree assessment of the probabilities of security breaches in computer systems, Proceedings of the 2nd Saudi Science Conference, Part Four:

Computer, Mathematics and Statistics, Jeddah, Saudi Arabia. 2014;1-17.

24. Zang X, Sun N, Trivedi KS. A BDD-based algorithm for reliability analysis of phased-mission systems. IEEE Transactions on Reliability. 1999;48(1):50-60.

25. Xing L. An efficient binary-decision-diagram-based approach for network reliability and sensitivity analysis. IEEE transactions on systems, man, and cybernetics-Part A: Systems and Humans. 2007;38(1):105-115.

26. Rauzy A. Binary decision diagrams for reliability studies. Chapter 25 in Misra, K.B. (Editor). Handbook of Performability Engineering. Springer, London, UK. 2008;381-396.

27. Mo Y. New insights into the BDD-based reliability analysis of phased-mission systems. IEEE Transactions on Reliability. 2009;58(4):667-678.

28. Rushdi AM, Rushdi MA. Switching-algebraic analysis of system reliability. Chapter 6 in M. Ram, M and P. Davim (Editors). Advances in Reliability and System Engineering. Springer International Publishing, Cham, Switzerland. 2017;139-161.

29. Rushdi AM, Ghaleb FA. A tutorial exposition of semi-tensor products of matrices with a stress on their representation of Boolean functions. Journal of King Abdulaziz University: Computing and Information Technology Sciences. 2016;5(1):3-30.

30. Rushdi AM, Bjaili HA. An ROBDD algorithm for the reliability of double-threshold systems, Journal of Advances in Mathematics and Computer Science. 2016;19(6):1-17.

31. Rushdi AM, Alturki AM. Computation of k-out-of-n system reliability via reduced ordered binary decision diagrams, Journal of Advances in Mathematics and Computer Science. 2017;22(3):1-9.

32. Rushdi AM, AM Alturki. Unification of mathematical concepts and algorithms of k-out-of-n system reliability: A perspective of improved disjoint products. Journal of Engineering Research. 2018;6(4):1-31.

33. Rushdi AM. Utilization of symmetric switching functions in the computation of k-out-of-n system reliability. Microelectronics and Reliability. 1986;26(5):973-987.

34. Rushdi AM. Reliability of k-out-of-n Systems. Chapter 5 in K. B. Misra, New trends in system reliability evaluation,

fundamental studies in engineering, Elsevier science publishers, Amsterdam, The Netherlands. 1993;16:185-227.

35. Rushdi AM. Partially-redundant systems: Examples, reliability, and life expectancy. International Magazine on Advances in Computer Science and Telecommunications. 2010;1(1):1-13.

36. Rushdi AM. Utilization of symmetric switching functions in the symbolic reliability analysis of multi-state k-out-of-n systems. International Journal of Mathematical, Engineering and Management Sciences (IJMEMS). 2019; 4(2):306-326.

37. Wong E, Eisenberg E. Iterative synthesis of threshold functions. Journal of Mathematical Analysis and Applications. 1965;11:226-235.

38. Winder RO. Enumeration of seven-argument threshold functions. IEEE Transactions on Electronic Computers. 1965;14(3):315-25.

39. Muroga S, Tsuboi T, Baugh CR. Enumeration of threshold functions of eight variables. IEEE Transactions on Computers. 1970;100(9):818-825.

40. Srivatsa SK, Biswas NN. Karnaugh map analysis and synthesis of threshold functions. International Journal of Systems Science. 1977;8(12):1385-1399.

41. Subramanian S, Thiagarajan B, Homaifar A. A novel approach to synthesis of threshold functions. In 1993 (25th) IEEE Southeastern Symposium on System Theory. 1993;200-204.

42. Gowda T, Leshner S, Vrudhula S, Konjevod G. Synthesis of threshold logic circuits using tree matching. In 2007 (18th) IEEE European Conference on Circuit Theory and Design 2007;850-853.

43. Gowda T, Vrudhula S, Kulkarni N, Berezowski K. Identification of threshold functions and synthesis of threshold networks. IEEE Transactions on Computer-Aided Design of Integrated Circuits and Systems. 2011;30(5):665-677.

44. Neutzling A, Martins MG, Ribas RP, Reis AI. Synthesis of threshold logic gates to nanoelectronics. In 2013 (26th) IEEE Symposium on Integrated Circuits and Systems Design (SBCCI). 2013;1-6.

45. Chen YC, Wang R, Chang YP. Fast synthesis of threshold logic networks with optimization. In 2016 (21st) IEEE Asia and South Pacific Design Automation Conference (ASP-DAC). 2016;486-491.

46. Neutzling A, Matos JM, Mishchenko A, Reis A, Ribas RP. Effective logic synthesis for threshold logic circuit design. IEEE Transactions on Computer-Aided Design of Integrated Circuits and Systems. 2018;38(5):926-937.

47. Moore EF, Shannon CE. Reliable circuits using less reliable relays. Journal of the Franklin Institute. 1956;262(3):191-208.

48. Burton RM, Howard GT. Optimal system reliability for a mixed series and parallel structure. Journal of Mathematical Analysis and Applications. 1969;28(2):370-382.

49. Misra KB. Reliability optimization of a series-parallel system. IEEE Transactions on Reliability. 1972;21(4):230-238.

50. Lin PM, Leon BJ, Huang TC. A new algorithm for symbolic system reliability analysis. IEEE Transactions on Reliability. 1976;25(1):2-15.

51. Chang EY, Thompson WE. Bayes analysis of reliability for complex systems. Operations Research. 1976;24(1):156-168.

52. Rushdi AM, Al-Khateeb DL. A review of methods for system reliability analysis: A Karnaugh map perspective, Proceedings of the First Saudi Engineering Conference, Jeddah, Saudi Arabia. 1983;1:57–95.

53. Rushdi AM, Hassan AK. Reliability of migration between habitat patches with heterogeneous ecological corridors. Ecological modeling. 2015;304:1-10.